Biol. Cybern. 79, 87–96 (1998)

Biological Cybernetics

Stimulus-induced bifurcations in discrete-time neural oscillators

Ali A. Minai, Tirunelveli Anand

Complex Adaptive Systems Laboratory, Department of Electrical & Computer Engineering and Computer Science, University of Cincinnati, Cincinnati, OH 45221-0030, USA

Received: 7 August 1997 / Accepted in revised form: 22 April 1998

Abstract. Based on theoretical issues and neurobiological evidence, considerable interest has recently focused on dynamic computational elements in neural systems. Such elements respond to stimuli by altering their dynamical behavior rather than by changing a scalar output. In particular, neural oscillators capable of chaotic dynamics represent a potentially very rich substrate for complex spatiotemporal information processing. However, the response properties of such systems must be studied in detail before they can be used as computational elements in neural models. In this paper, we focus on the response of a very simple discrete-time neural oscillator model to a fixed input. We show that the oscillator responds to the stimulus through a fairly complex set of bifurcations, and shows critical switching between attractors. This information can be used to construct very sophisticated dynamic computational elements with well-understood response properties. Examples of such elements are presented in the paper. We end with a brief discussion of simple architectures for networks of dynamical elements, and the relevance of our results to neurobiological models.

1 Introduction

In the computational neurobiology literature there is increasing focus on spatiotemporal rather than simply spatial patterns for representation and processing of cognitive information. For example, the well-known correlation theory developed by von der Malsburg and colleagues (von der Malsburg and Schneider 1986; von der Malsburg and Buhmann 1992) hypothesizes that the visual system uses temporal correlation between neurons' activity for representing sensory features. This theory has received considerable support from physiological experiments (Eckhorn et al. 1988; Gray et al. 1989; Engel et al. 1991a,b), and has been elaborated further by other researchers (König and Schillen 1991; Schillen and König 1991; Hansel and Sompolinsky 1992; Wang and Terman 1995; Campbell and Wang 1996). There is also significant evidence that the olfactory system encodes and classifies stimuli by altering its dynamics rather than by converging to a static pattern (Freeman 1979; Skarda and Freeman 1987; Yao and Freeman 1990). Thus, it is of interest to consider computational elements that encode information and respond to it by altering their dynamical behavior rather than just the magnitude of their output.

Most computational neuroscience models with dynamic neural elements have focused on spiking dynamics, motivated by the seminal model of Hodgkin and Huxley (1952) and its derivatives. However, there has also been considerable interest in the behavior of neural populations (Abeles 1991). In a seminal paper, Wilson and Cowan (1972) developed an oscillator model to describe interacting populations of excitatory and inhibitory neurons, and this has formed the basis of many subsequent models of cognitive information processing (Baird 1986; Campbell and Wang 1996). Systems of neural oscillators representing interacting neural populations have also been used as models of pattern formation and spatiotemporal self-organization (Murray 1989).

In the physics literature there is a large body of work on the behavior of interacting oscillators, particularly with regard to synchronization between chaotic oscillators (Pecora and Carroll 1990, 1991; Hansel and Sompolinsky 1992; He and Vaidya 1992; Carroll and Pecora 1993; Brown et al. 1994; Abarbanel et al. 1996; Malescio, 1996; Morgül and Feki 1997). Much larger scale systems of interacting oscillators have also been studied from a phenomenological point of view (Kaneko 1989, 1990), and several researchers have explored applications for networks of coupled neural oscillators (Aihara et al. 1990; Ishii et al. 1996; Adachi and Aihara 1997).

Most of the work on neural oscillators has focused on continuous-time models – like the Wilson-Cowan model – with two phase variables. Relatively little attention has been paid to discrete-time models, though their behavior

Correspondance to: A. A. Minai

often differs fundamentally from their continuous-time counterparts. The work reported in this paper focuses on a very simple class of oscillators introduced by Xin Wang (1991, 1992) which is similar in form to the Wilson-Cowan model, albeit with discrete-time dynamics. Because of their discrete-time nature, these very simple oscillators – termed *Wang oscillators* or *W-oscillators* in this paper – can produce dynamical behaviors ranging from fixed points through quasiperiodicity to chaos (Wang 1991, 1992). While the intrinsic dynamics of these oscillators are well understood, if they are to be used as models of computational elements, an understanding of their response to external stimuli is also essential. That is the focus of this paper.

2 Mathematical description

The Wang oscillator described by Xin Wang (1991, 1992) essentially models the interaction of two nonlinear elements, one excitatory and the other inhibitory. The elements can be seen as representing single neurons, but are best thought of as populations of neurons. The equations for the oscillator are:

$$x^{t+1} = f(w_{xx}x^t - w_{xy}y^t + u^{t+1} - \theta_x) \tag{1}$$

$$y^{t+1} = f(w_{yx}x^t - w_{yy}y^t + v^{t+1} - \theta_y) \tag{2}$$

where t is the time index, x^t and y^t are the two state variables, the w's are weight parameters, u^t and v^t are external inputs, θ are fixed thresholds, and $f(\,)$ is a sigmoid function. We take $f(p;\mu) = \tanh(\mu p)$, and $\theta_x = \theta_y = 0$. We also assume $w_{xx} = w_{xy} = a$ and $w_{yx} = w_{yy} = b$, so a and b can be thought of as intrinsic gain factors for the excitatory and inhibitory units, respectively. Wang (1991) has shown that, with $a \geq 2b$ and $u^t = v^t = 0$, changing μ produces a series of period-doubling bifurcations to chaos. In fact, other values can also lead to chaos, but this will not be discussed further in this paper. In all analysis and simulations presented in this paper, we assume that $a \geq 2b$. The possible biological significance of this condition is discussed in Sect. 6.

With the specification of $f(\,)$ and the restriction of weights, the oscillator can be written as a discrete-time map of the single state variable, $z^t = x^t - y^t$, with (possibly time-varying) inputs u^t and v^t:

$$z^{t+1} \equiv F(z^t) = \tanh[\mu(az^t + u^{t+1})] - \tanh[\mu(bz^t + v^{t+1})] \tag{3}$$

Consider first the case when there are no external inputs: $u = v = 0$. For fixed a and b with $a \geq 2b$, one can obtain the period-doubling cascade to chaos for z^t by increasing μ. For small μ, the origin is a stable fixed point, but it loses stability when $|\mu(a-b)| > 1$, initiating the period-doubling cascade. Clearly, all of z's dynamics occurs in the $(-2, 2)$ interval of the real line, though $F : z^t \to z^{t+1}$ is defined over the whole real line. For $u = v = 0$, the odd symmetry of $F(z)$ about the origin creates two distinct basins of attraction: (1) Z^+, where $z^t > 0$ and (2) Z^-, where $z^t < 0 \;\; \forall t > t'$. There is a complete period doubling cascade in each basin. Thus, for any given $\mu > |a-b|^{-1}$, there are two attractors: ζ^+ for Z^+ and ζ^- for Z^-. In this situation and with no external input, $z = 0$ is an unstable fixed point of the dynamics, all positive states/initial conditions are in Z^+ and all negative ones are in Z^-. However, in the presence of an input, the map becomes more complicated and the basins depend also on the input.

In the following section, we consider the response of a W-oscillator in its chaotic phase to a fixed input.

3 Dynamics of the W-oscillator with fixed input

To study the response of the oscillator to an external fixed input, we set $u^t = u$ and $v^t = 0$. Thus, the dynamics of the oscillator follows

$$z^{t+1} \equiv F_u(z^t) = \tanh[\mu(az^t + u)] - \tanh[\mu b z^t] \tag{4}$$

We term this a $\mu/a/b$ oscillator. The only effect of $u \neq 0$ is to shift the positive $\tanh(\,)$ function by u; which causes the zero-crossing of $F_u(z)$ to shift by $\delta = u/(b-a)$ (Fig. 1). This clearly changes the dynamics of z, albeit in a highly nonlinear way. The main question is: how does the input, u, affect the long-term dynamics of z? It turns out that four types of bifurcations occur as $|u|$ is increased: (1) a tangent (saddle-node) bifurcation; (2) a crisis; (3) a reverse crisis; and (4) reverse period doubling bifurcations. This is not unexpected, since each half of $f(z)$ is similar to a logistic map (Wang, 1991) and subject to the same bifurcations. However, in this instance, the bifurcation parameter is the external input, and the dynamics is bounded over the $(-\infty, +\infty)$ interval. Thus, crises and saddle node bifurcations lead to attractor flipping rather than instability, creating the potential for a significantly more complex bifurcation pattern than that seen for the logistic map.

Consider the $u \leq 0$ case with a, b, and μ set such that the $F_0(\,)$ map is chaotic. If the initial condition (IC) is $z^0 < 0$, all trajectories are in Z^-, and the effect of increasing $|u|$ is to produce a cascade of period halving bifurcations. As $u \to -\infty$, $F_u(z) \to -1 - \tanh[\mu b z]$, which has a period-2 attractor if μb is large enough for $F_0(\,)$ to be chaotic. In this case, therefore, no $|u|$ is large enough to produce a fixed point in the Z^- basin for $u < 0$.

The bifurcation behavior of $F_u(\,)$ for the $u \leq 0$ case is much more complex for $z^0 > 0$. On the $z \geq 0$ axis, define $z_l = z : F_u(z) = z, F_u'(z) > 0$, and $z_u = z : F_u(z) = z_l$, $F_u'(z) < 0$, denote the interval $[z_l, z_u]$ by T, and the complementary interval $(-\infty, z_l) \cup (z_u, \infty)$ by T'. Here, $F_u'(z)$ is the derivative of F_u with respect to z. On the $F_u(z) \geq 0$ axis, define $\xi_l = z_l$ and $\xi_u = \max_z[F_u(z)]$. All of these are shown in Fig. 2. Note that z_l, if it exists, is an unstable fixed point of $F_u(\,)$. Thus, all $z^0 < z_l$ are in the Z^- basin, as are all $z^0 > z^u$, since they map to $z < z_l$ after one time step. What about initial conditions in T?

Clearly, if $|z_u - z_l| \geq |\xi_u - \xi_l|$, $z \in T \Rightarrow F(z) \in T$, i.e., T is a *trapping region* for the dynamics. Any trajectory

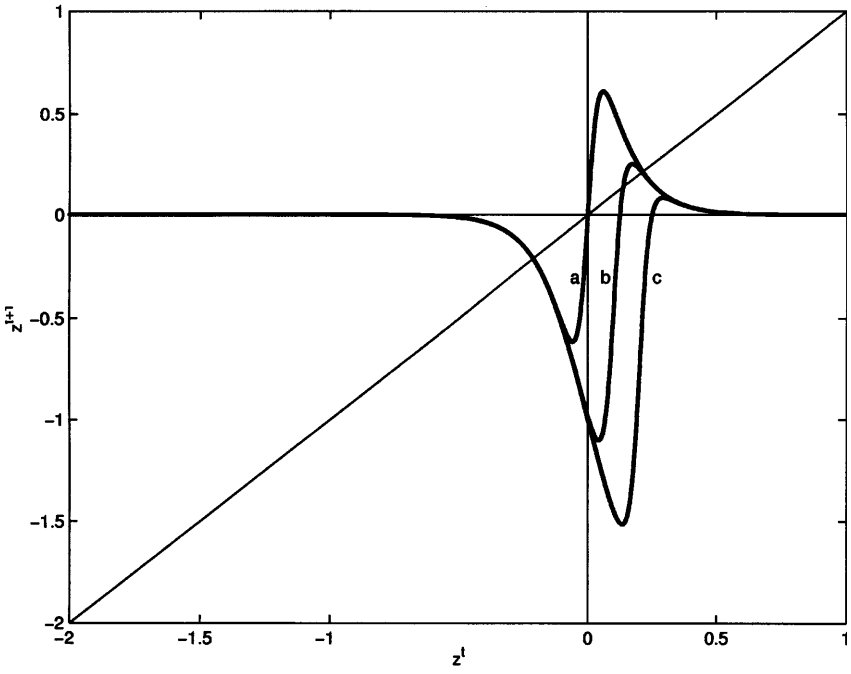

Fig. 1. The $F_u : z^t \to z^{t+1}$ map for $u = 0$ (a), $u = -0.5$ (b), and $u = -1.0$ (c). In all cases, $\mu = 5.0$, $a = 5.0$, and $b = 1.0$

starting in T remains in T, and its dynamics converges to the attractor corresponding to Z^+. In contrast, if $|z_u - z_l| < |\xi_u - \xi_l|$, T is not a trapping region (Fig. 2), and the Z^+ basin virtually disappears – the set of states in T that converge to $z_l \in T$ form a Cantor set (see, for example, Peitgen et al. 1992). Thus, the following can be stated for the $u < 0$ case:

1. If $z_u > \xi_u$, Z^+ corresponds to $T = [z_l, z_u]$, and Z^- to T'.
2. If $z_u < \xi_u$, almost all states are in Z^-.

The significance of Z^+ and Z^- is reversed for $u > 0$.

For $u = 0$, $z_l = 0$, $z_u = \infty$, and $\xi_u < 1$, so that condition (1) applies with $T = [0, \infty)$. As $|u|$ increases, both ξ_u and z_u decrease monotonically. However, the decrease in ξ_u is slow, while that in z_u is very rapid, essentially moving up the tail of $F_u(\,)$. There are two points of intersection for z_u and ξ_u as functions of u. These are denoted by u_1^* and u_2^*, with $|u_1^*| < |u_2^*|$. Trapping regions exist for $|u| < |u_1^*|$ and $|u| > |u_2^*|$. There is also a point of tangency, u', where $F_u(z)$ falls below the diagonal, causing a tangent bifurcation. Since the maximum of $F_u(\,)$ is approximately quadratic,

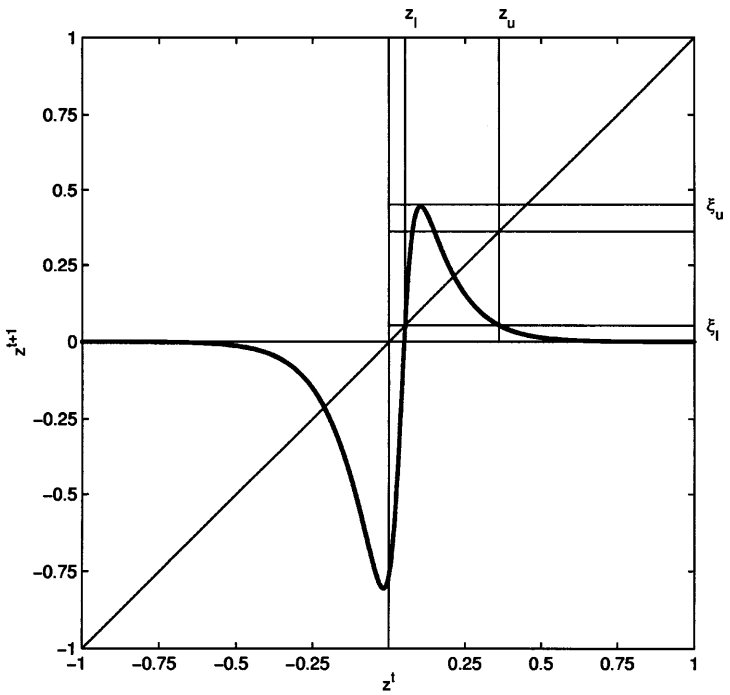

Fig. 2. The z_l, z_u, ξ_l, and ξ_u parameters for the $F_u(z)$ map with $u = -0.2$, $\mu = 5.0$, $a = 5.0$, and $b = 1.0$

$|z_u - z_l| > |\xi_u - \xi_l|$ near the point of tangency, implying that $|u_2^*| < |u'|$. However, $|u' - u_2^*| \to 0$ as μa increases. Figure 3 shows the numerically calculated values of all the relevant parameters for a 5/5/1 oscillator with $u < 0$.

Qualitatively, the bifurcation process for $z^0 > 0$, $u \leq 0$ can be described as follows. As $|u|$ increases from 0, a standard period-halving cascade begins in the rapidly shrinking trapping region for Z^+, while initial conditions outside the trapping region move to Z^-. However, at $u = u_1^*$, the trapping region disappears abruptly as z_u falls below ξ_u. This is a crisis (Grebogi et al. 1983), which interrupts the period-halving, and almost all initial conditions move into the Z^- basin. Then, at $u = u_2^*$, the trapping region reappears as z_u again overtakes ξ_u. This is a reverse crisis. The Z^+ basin reappears for $z^0 \in T$, and the period halving resumes for ICs in the trapping region. Finally, the tangent bifurcation occurs at $u = u'$, and all initial conditions fall back into the Z^- basin.

Overall, the response of the oscillator to external inputs between $\pm\infty$ can be divided into eight regions symmetric around the $u = 0$ axis (Fig. 4).

1. Regions I and VIII ($|u| > |u'|$). These are the outermost regions, and the sign of the attractor is identical to that of the input, while its quality (cycle of period k or chaos) is determined by the input's magnitude. The inner ends of these regions mark the tangent bifurcations.
2. Regions II and VII ($|u'| < |u| < |u_2^*|$). In these regions the attractor for most ICs has the sign of the input, but for a restricted set, T, of initial conditions, the response takes the sign of the IC. The inner ends of these regions mark the reverse crises.
3. Regions III and VI ($|u_2^*| < |u| < |u_1^*|$). These regions lie between the crisis at u_1^* and the reverse crisis at u_2^*, and the sign of the attractor for all but a Cantor set of initial conditions is identical to that of the input.
4. Regions IV and V ($|u| < |u_1^*|$). In these regions the sign of the attractor for initial conditions in T is the same as that of the IC, which creates *hysteresis* in the oscillator's switching in response to u. The extent of the trapping region on the state axis increases rapidly as the input approaches 0, so that one can always find an input small enough to trap any initial condition. Indeed, the situation at $u = 0$ can be seen as the limiting case where all ICs are 'trapped' in the basin corresponding to their sign.

A comparison of Fig. 4a with Fig. 3 will illustrate the correspondences between the various bifurcations and parameters for $u \leq 0$.

4 Information processing in W-oscillators

In essence, information processing is the ability to represent, transform, and discriminate. One of the simplest (and most useful) information processing elements is a switching device which responds to stimuli by switching into one of two states. Such devices have, of course, formed the basis of many neural network models (Hopfield 1982; Hertz et al. 1991). More sophisticated devices respond to stimuli in a gradual manner, e.g., by producing real-valued output as in standard sigmoid neurons or radial-basis function units.

Since it has two basins of attraction in input space, a W-oscillator can clearly serve as a switching device. However, it can also produce a finer gradation of response by changing the *quality* of its dynamics. In Sect. 6

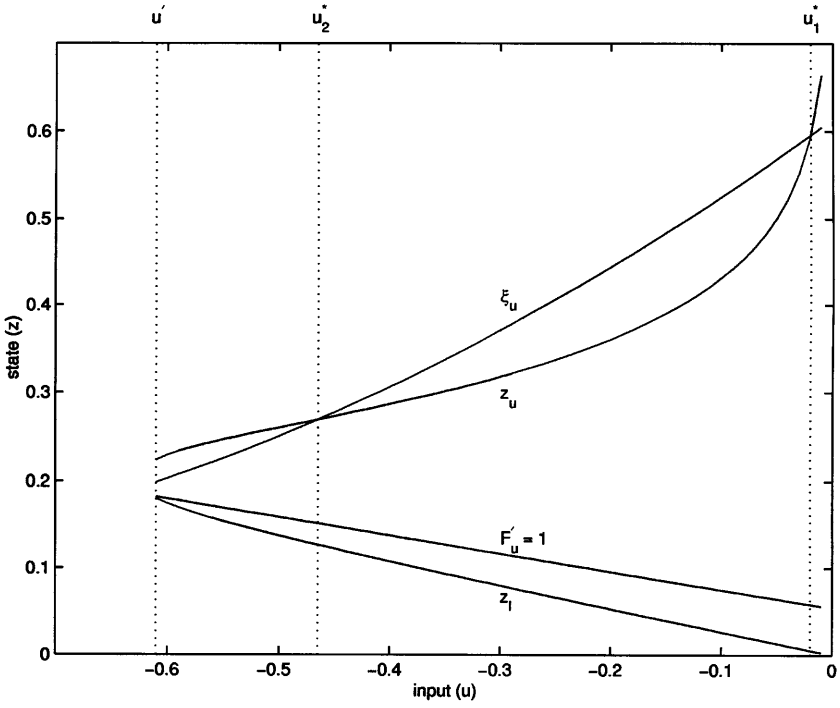

Fig. 3. Numerically calculated values of the z_l, z_u, $\xi_l (= z_1)$, and ξ_u parameters for a 5/5/1 oscillator. The $F'_u = 1$ curve is also drawn to determine the point of tangency. The three bifurcation points are indicated by the *dotted lines*. Note that, for $|u| < |u_1^*|$ and $|u'| > |u| > |u_2^*|$, the trapping region lies between the z_l and z_u curves. For $|u| > |u'|$, only the Z^- basin exists

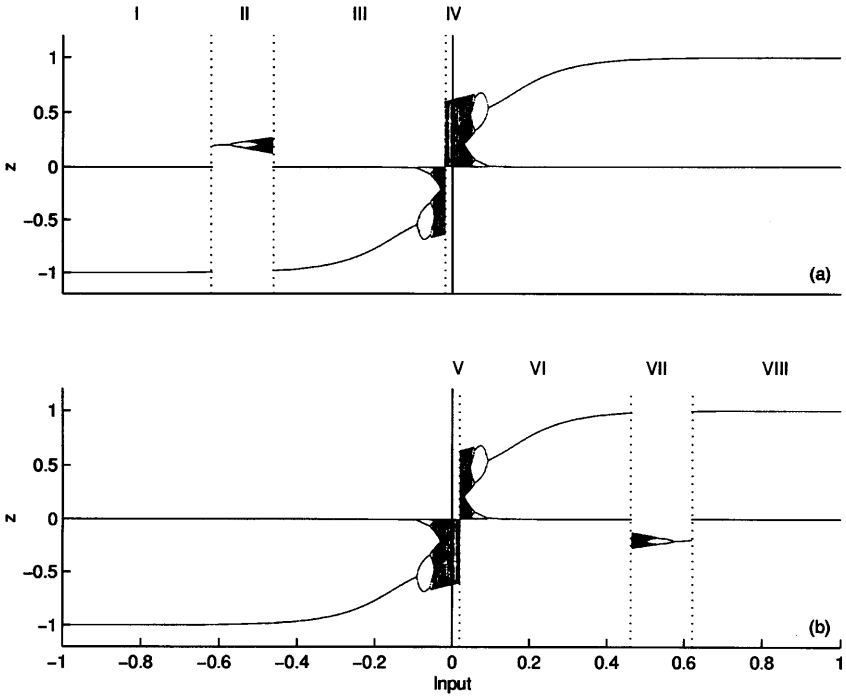

Fig. 4a,b. The eight regions of the bifurcation diagram for a 5/5/1 oscillator. **a** shows the bifurcation diagram for $z^0 = 0.2$, while **b** shows the one for $z^0 = -0.2$. This initial condition was chosen because it lies in the trapping regions in both zones IV–V and II–VII. Other initial conditions may not show trapping in these zones

we discuss how the variables and parameters of the model described in (1), (2) and (3) correspond to physical and physiological quantities. Here, we briefly note that the state variables, x^t and y^t, can be seen as representing the *aggregate activities* of excitatory and inhibitory neuronal populations (Wilson and Cowan 1972), while input u corresponds to an external stimulus, such as a sensory signal or feature. The response of the system to the intensity of the stimulus constitutes a *dynamical representation* of the stimulus. For example, when u is small (which may correspond to a weak stimulus), z^t remains chaotic, implying that x^t and y^t are chaotic too. This indicates complex, aperiodic dynamics in the underlying neurons in each population. When u increases, the dynamics of x^t and y^t becomes periodic, which can be interpreted as coherent, phase-locked periodic activity within each population. Thus, a simple interpretation of x^t and y^t moving from chaos to periodicity is in terms of increased phase-coherence between neurons in each population. This dependence of synchrony on stimulus strength is precisely the type of effect some have proposed for information processing in the brain (Freeman 1979; von der Malsburg and Schneider 1986; Skarda and Freeman 1987; Eckhorn et al. 1988; Gray et al. 1989; Yao and Freeman 1990; Engel et al. 1991a,b; König and Schillen 1991; Schillen and König 1991; Hansel and Sompolinsky 1992; von der Malsburg and Buhmann 1992; Wang and Terman 1995; Campbell and Wang 1996).

In the rest of this section we discuss how the oscillator model described above can be used for information processing in the sense of representing stimulus intensity (or even quality) through changes in system dynamics. This dynamics, in turn, corresponds to global behaviors of implicit neuronal populations underlying the aggregate oscillator model discussed here.

It follows from the analysis above that for an oscillator to switch with the sign of the stimulus would require two things: (1) elimination of regions IV and V; and (2) elimination of regions II and VII. The latter can be achieved by the constraint $|u| < |u_2^*|$. The problem can also be minimized by choosing μa large enough that $|u'| \approx |u_2^*|$. The elimination of regions IV and V can be achieved also by eliminating the corresponding input values. One way to do this is to modify the input to $\bar{u} = u + \epsilon \mathrm{sgn}(u)$, where $\epsilon > |u_1^*|$. The result is an oscillator whose response polarity is determined by the sign and response quality by the magnitude of its input. In some situations it may be of benefit to retain the hysteresis provided by regions IV and V, so that small inputs do not cause switching.

The most notable feature of the oscillator described above is that it functions as a threshold unit but, unlike sigmoids, etc., maps the magnitude of its input to different dynamic response patterns rather than to static scalar values. Since the unit responds to its input through bifurcation, we term it a *bifurcational threshold unit* (BTU). As the input, u, is a lumped scalar value, very complex dynamic response characteristics can be constructed over a multi-dimensional feature space by using appropriate composition functions. To this end, we specify a general form for the input to the oscillator as:

$$u = g(\lambda) + \epsilon \mathrm{sgn}(g(\lambda)) \tag{5}$$

$$\lambda = h(s) \tag{6}$$

where s is a vector in some m-dimensional input feature space, $\Sigma^m \subset R^m$, $g(\,)$ is a modifying function, and $h(\,)$ is a composition function, e.g., $h = Ws$, where W is a weight vector. In neurobiological terms, $h(\,)$ and $g(\,)$ could be seen as representing the integration and (possibly

nonlinear) filtering of afferent input in the dendrites of the excitatory neuronal population. Of course, in non-biological networks, the forms of $h(\,)$ and $g(\,)$ would be chosen according to the application rather than biological plausibility.

Figure 5 shows the response of a 5/5/1 BTU over a one-dimensional input space for $h(x) = x$, and (a) $g(x) = 0.01x$, and (b) $g(x) = 0.01\sin(10x)$. Thus, in (a), $g(x)$ is just a simple, linear gain, while in (b) it is a nonlinear transformation – perhaps suitable for detecting some periodic structure in the input. Clearly, there is great scope for producing highly structured but complex dynamic response patterns by controlling $g(\,)$.

As an example of the type of processing possible, consider a unit, i, with m inputs, $s_j \in (-1, +1)$, defined by the following equations:

$$\lambda_i = \sum_{j=1}^{m} w_{ij} s_j = Ws \tag{7}$$

$$u_i = A_i \lambda_i + \epsilon_i \mathrm{sgn}(A_i \lambda_i) \tag{8}$$

$$z_i^{t+1} = F_{u_i}(z_i^t) \tag{9}$$

where s_j is the jth input, w_{ij} is the weight from the jth input to the unit, and A_i and ϵ_i are parameters. Such a unit will be termed a linear BTU (LBTU). For input vectors with small $|Ws|$ (i.e., little similarity between s and fixed weight vector, W), the unit will receive a small input which, with appropriately chosen A_i and ϵ_i, will result in a chaotic response. An input more similar to W would produce a cyclic response whose period and amplitude depend on $|Ws|$. Thus, the LBTU would encode the similarity of its input with its stored weight vector by means of bifurcation, producing a relatively unstructured (chaotic), weak, and unrepeatable response for stimuli it does not recognize, and a highly structured (periodic), stronger, and totally repeatable response for stimuli it does recognize. Figure 6 shows the response of a 5/5/1 LBTU with a unit length weight vector and $\epsilon_i = 0.02$ to a two-dimensional unit length input vector under two different settings of A_i. By using a radial function for λ_i, the BTU can be made sensitive to distance from W instead of the projection.

5 Networks of BTUs

Clearly, BTUs can be used as elements in a variety of network architectures analogous to standard neural networks. An extremely simple case in point is a network that is a layer of N unconnected LBTUs, i, as defined in Eqs. (7)–(9), with weight vectors, W_i, set by a standard unsupervised learning method (Kohonen 1984). If an input pattern, s^k, is given as stimulus to this network, those neurons which have high $W_i s^k$ values – i.e., those which 'recognize' the pattern – show a periodic response, while those that do not recognize the pattern remain chaotic. If the pattern is novel, and no neuron recognizes it, the whole network remains chaotic. The degree to which a pattern is recognized by the network can then be represented dynamically by the phase space behavior of the z^t vector (Fig. 7). This response is very similar to that reported in the olfactory system by Freeman and colleagues (Skarda and Freeman 1987; Yao and Freeman 1990), where the system is in high-dimensional chaos during the resting state or when given a novel input odor, and recognition of a familiar odor is signaled by a reduction in the dimension of the attractor. Of course, the olfactory model network has much more complex functionality arising from its more sophisticated structure.

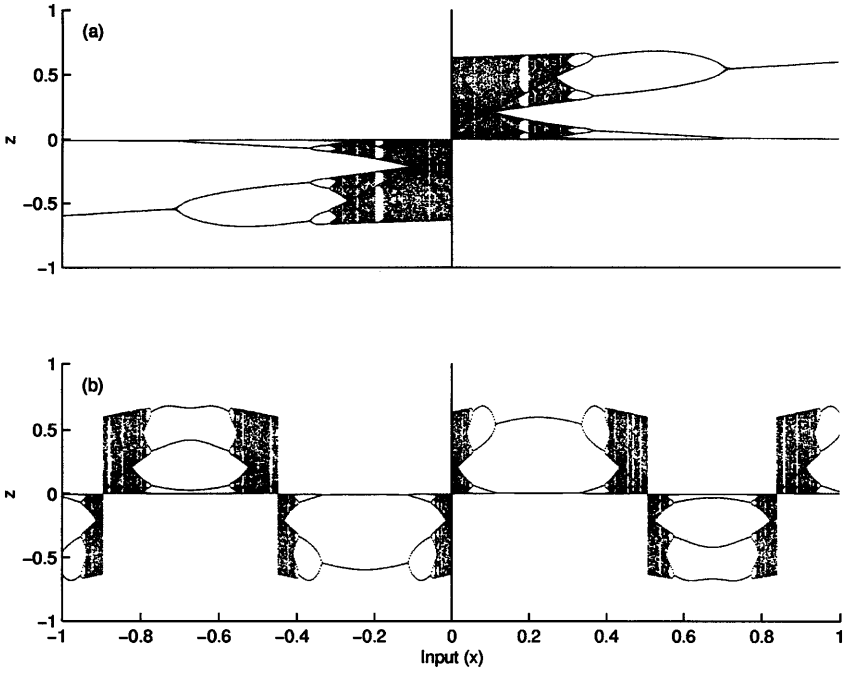

Fig. 5a,b. Bifurcation diagrams for two 5/5/1 BTUs. In **a**, $u = 0.01x + 0.05\mathrm{sgn}[0.01x]$, and in **b**, $u = 0.01\sin(10x) + 0.05\mathrm{sgn}[0.01\sin(10x)]$, where $-1 \le x \le 1$. Input x may represent the intensity of a scalar quantity, or the strength of a feature.

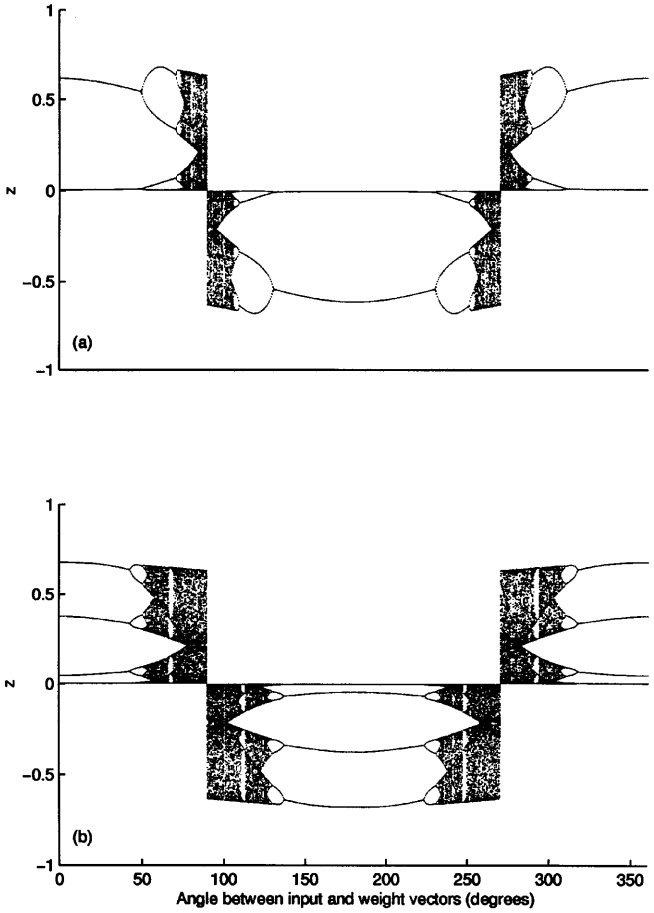

Fig. 6. Bifurcation diagrams for a 5/5/1 LBTU with a two-dimensional input and **a** $A_i = 0.11$, and **b** $A_i = 05$. The x-axis represents the angle between the weight vector of the LBTU and the input vector. The net input is determined as in Eqs. (7) and (8), with $\epsilon = 0.02$. The initial condition is $z^0 = -0.005$ for all cases

A Hopfield-type network (Hopfield 1982) can also be constructed from N BTUs to function as an associative memory which learns a set of patterns, $\xi^v \in \{0,1\}^N$. The equations for the BTUs are:

$$\lambda_i^{t+1} = \sum_{j \neq i} w_{ij} \operatorname{sgn}(z_j^t) \tag{10}$$

$$u_i^{t+1} = \lambda_i^{t+1} + \epsilon \operatorname{sgn}(\lambda_i^{t+1}) \tag{11}$$

$$z_i^{t+1} = F_{u_i^{t+1}}(z_i^t) \tag{12}$$

$$w_{ij} = \frac{\alpha}{N} \sum_v \xi_i^v \xi_j^v \tag{13}$$

where ϵ and $\alpha > 0$ are parameters set by the user. If the output of the network is taken to be $\operatorname{sgn}(z^t)$, the system is basically indistinguishable from a bipolar associative memory. However, each unit, i, can also be seen as encoding the certainty of its response by the dynamics of z_i^t: units with net input, λ_i, close to 0 (i.e., weakly polarized) are chaotic, while those with net input far from 0 (highly polarized) are in a low-period cycle.

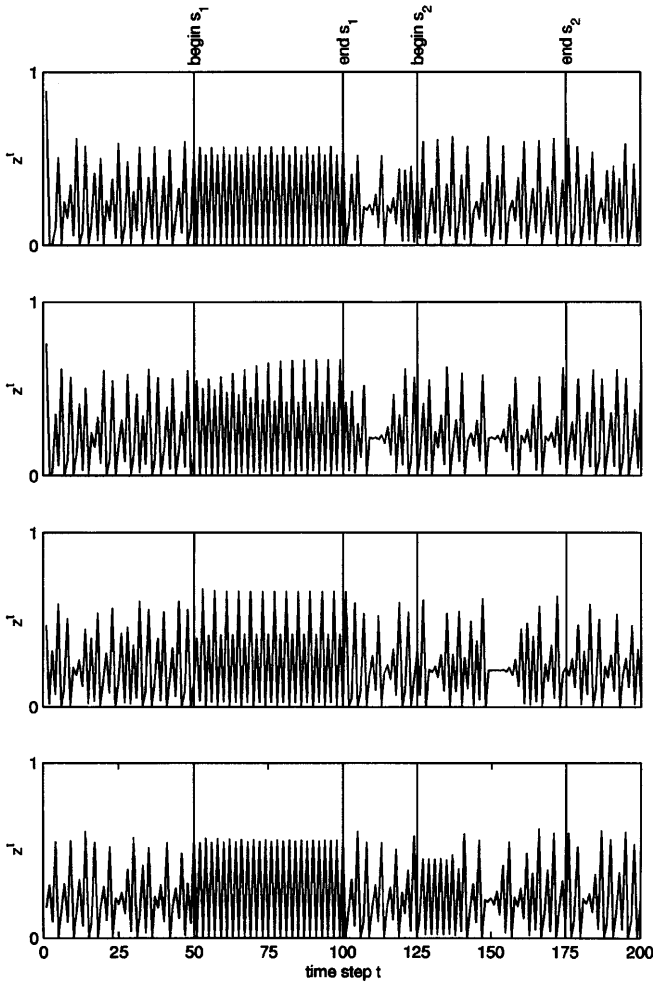

Fig. 7. The time series for a feed-forward single-layer network of four 5/5/1 LBTUs stimulated with patterns s_1 (steps 50–100) and s_2 (steps 125–175). Each oscillator gets the same four-dimensional stimulus. The weight vectors of all oscillators are oriented close to pattern s_1 and far from stimulus s_2. Note the difference in response to the two stimuli, based on recognition. Essentially, the network transforms the static patterns into dynamic responses, differentiating between those it recognizes and those it does not

In general, networks capable of performing difficult information processing tasks will need to be more complex than the examples given above. Networks of interconnected BTUs especially offer interesting possibilities, some of which were explored phenomenologically by Wang (1992). However, a deep understanding of such networks requires a systematic study of how W-oscillators respond to time-varying inputs of various classes. We have reported elsewhere that stochastic inputs to identical W-oscillators can lead to rapid synchronization (Minai and Anand 1998a,b), which may have applications in areas such as cryptography and communication (Minai and Pandian 1998). More results will be reported in future papers.

6 Biological considerations

The analysis and discussion above has been purely at an abstract level, but the conclusions have important

consequences for mathematical models of neural populations. Consider two populations of neurons – an excitatory population with global activity denoted by X_E^t, and an inhibitory population with global activity X_I^t. Both populations have sigmoid response functions (Wilson and Cowan 1972),

$$X_E^t = \frac{1}{1+\exp(-k_E Y_E^t + \Theta_E)} \tag{14}$$

$$X_I^t = \frac{1}{1+\exp(-k_I Y_I^t + \Theta_I)} \tag{15}$$

where k_E and k_I are gain parameters, Θ_E and Θ_I are biases, and Y_E^t and Y_I^t the net inputs for the excitatory and inhibitory populations, respectively. The populations interact reciprocally with identical weights and the excitatory population also receives an external stimulus, U^t, so that $Y_E^{t+1} = X_E^t - X_I^t + U^{t+1}$, and $Y_I^{t+1} = X_E^t - X_I^t$. The difference in activity between the two populations can then be written as

$$\begin{aligned} Z^{t+1} &\equiv X_E^{t+1} - X_I^{t+1} \\ &= \frac{1}{2}\left\{\tanh\left[\frac{k_E}{2}(X_E^t - X_I^t + U^{t+1}) - \frac{\Theta_E}{2}\right]\right. \\ &\quad \left. - \tanh\left[\frac{k_I}{2}(X_E^t - X_I^t) - \frac{\Theta_I}{2}\right]\right\} \end{aligned} \tag{16}$$

which is identical to (3) except for the $1/2$ multiplier if we take $\mu a = k_E/2$, $\mu b = k_I/2$, $u^t = aU^t$, and $\Theta_E = \Theta_I = 0$. Thus, the analysis given above – including that on stimulus-induced bifurcations – holds for interacting neural populations under reasonable modeling assumptions.

It should be noted that the range of behaviors described for the differential activity, Z^t, appears also in the activities, X_E^t and X_I^t, of the individual populations (Wang 1992). Thus, the variables of our model, x^t, y^t, and u^t, have immediate interpretations as physical and physiological quantities. Going back to (1) and (2) and setting $w_{xx} = w_{xy} = a$, $w_{yx} = w_{yy} = b$, $v^t = 0$, and $f(\,) = \tanh(x;\mu)$, we can write:

$$x^{t+1} = \tanh[\mu(a(x^t - y^t) + u^{t+1} - \theta_x)] \tag{17}$$

$$y^{t+1} = \tanh[\mu(b(x^t - y^t) - \theta_y)] \tag{18}$$

Thus, we have two neural populations – an excitatory one, with state x^t, and an inhibitory one with state y^t – connected reciprocally. The state variables represent the normalized activity of each population above and below some average level (Eeckman and Freeman 1986). Parameters μa and μb determine the intrinsic nonlinearity of response in the excitatory and inhibitory groups, respectively. Thus, the condition $a \geq 2b$ essentially states that the excitatory population responds in a much more nonlinear (i.e., threshold-like) manner than the inhibitory population. This has a clear analog in the case of real neuronal populations in, for example, regions CA3 and CA1 of the hippocampus. Physiological evidence suggests that inhibitory interneurons in CA3/CA1 respond to stimuli with multiple spikes whose number and onset latency is directly related to the strength of the stimulus (Fox and Ranck 1981; Buzsàki and Eidelberg 1982). This is in contrast to the excitatory neurons, which respond in an all-or-none fashion when their stimulus exceeds a threshold (Fox and Ranck 1981). Thus, groups of inhibitory neurons – at least in the hippocampus – have a much smoother population response function than excitatory neurons. This is essentially what the $a \geq 2b$ condition states. Of course, one should not read too much into the precise factor of 2, which is a consequence of the model, but interpret the condition as $a \gg b$, which is entirely consistent with our results. The smoothness of inhibitory response has been used previously in models of the hippocampus (Minai and Levy 1993, 1994; Levy 1996; Wu et al. 1996).

The u^t signal represents an external input to the excitatory population. As described in earlier sections, its value determines the quality of the system's dynamics. So, for example, u^t might code for the intensity of a sensory input (e.g., light, smell), or of some more complex sensory feature. The neural populations then represent this intensity by showing different degrees of complexity in behavior – ranging from chaotic behavior for weak stimulus to simple period-2 behavior for a strong stimulus. As discussed earlier, much more complex, perhaps non-monotonic, responses are also possible. It is important to keep in mind that states x^t and y^t are intended to represent aggregate behaviors, and, as discussed earlier, periodicity in these variables implies simple, phase-coherent dynamics of the underlying implicit neural elements.

One question that might arise here is whether the particular map we use in our model [Eqs. (3), (17) and (18)] has a special significance, or if any 'arbitrary' map with similar bifurcational properties could be used instead. Clearly, the formal behavior described could be obtained from other maps which show a similar pattern of bifurcation, but there is a strong reason for the choice we have made. The map we use is the difference of two sigmoid functions, where the sigmoids represent the response characteristics of each individual neuronal population. There is considerable theoretical and experimental support for sigmoidal response functions, both at the level of individual cells (Rall 1955) and cell assemblies (Wilson and Cowan 1972; Eeckman and Freeman 1986). In particular, it is well established that, given a population of threshold elements with unimodally distributed thresholds, the aggregate response has a sigmoidal form (Wilson and Cowan 1972; Levine 1991). As discussed above, while we use the bipolar $\tanh(\,)$ function for each neuronal population, our results apply equally to the map $f(x) = [1+\exp(-\mu x)]^{-1}$, which is strictly positive.

An interesting secondary property which also makes our map suitable for modeling neuronal populations is that the stimulus which produces the bifurcational response acts additively, which has been a standard assumption in neuronal modeling. In contrast, many other maps require changes in the value of a multiplicative

parameter to produce bifurcation (e.g., μ in our map). We submit that, while such parameters are crucial for modeling changes in system sensitivity, responsiveness, etc., they are unsuitable as models of additive external stimulus. Indeed, it is for this reason that we do not term u^t a parameter, but consider it a signal. The fact that the system bifurcates in response to an external signal rather than change in an internal parameter is precisely what makes the system useful as an information-processing device.

The additive nature of u^t also means that our analysis can also be used to understand how changes in threshold, Θ_E and Θ_I, affect the system. Another case of interest is when the response functions of the neural populations are not sigmoids but superpositions of several sigmoids, as when the neuron firing thresholds have multimodal distributions (Wilson and Cowan 1972). In this case, the function relating Z^{t+1} to Z^t would be considerably more complex than $F_u(z)$, but could be analyzed using methods similar to those used in this paper. The main consequence would be the creation of more attractors. Detailed analysis of this case will be addressed in future reports.

One interesting issue that arises from this study is how the discrete-time dynamics of the model studied here relates to that of similar continuous-time models such as the Wilson-Cowan oscillator. As is well known, the dynamics of low-dimensional discrete-time systems can be considerably more complex than continuous-time systems of the same dimension. The conditions under which the asymptotic behavior in the two cases can be matched have been studied by Wang and Blum (1992). Often, it is useful to see a discrete-time system as the Poincare map of a higher dimensional continuous-time system (Wang 1992; Doyon et al. 1993, 1994; Cessac et al. 1994). However, in the context of some neural systems, such as the hippocampus, this can be given an especially simple interpretation. As is well known, the excitability of neurons in the hippocampus is phase-locked to the 5–12 Hz theta rhythm (Buzsáki et al. 1983; Fox et al. 1986). There is also evidence that the sampling of olfactory stimuli by rodents is synchronized with the theta oscillation (Macrides et al. 1982). Thus, even though the system operates in continuous time, it can be seen computationally as a discrete-time system – or, alternatively, as a Poincare map of the higher-dimensional system which includes the phase of the theta rhythm as a phase variable.

As a counterpoint to the discussion in this section, it should be noted that information processing in highly distributed nonlinear systems poses very difficult questions which are unlikely to have simple answers. Models and methods such as those we describe in this paper are aimed at exploring simple principles which may underlie the complexity of actual neural information processing. The complementary need for elucidating detailed neurodynamical processes and relating them to each other remains an important challenge to those who seek a computational understanding of the nervous system.

To conclude, we have shown that the qualitative dynamics of interacting inhibitory and excitatory neural populations can range from chaos to limit cycle behavior as the external stimulus to the excitatory population is varied. The system can be switched between two attractors by the polarity of the stimulus. Several types of bifurcations, including crises, period-halving, and tangent bifurcations, can occur, and the system can exhibit hysteresis in its response to the input. The interacting populations, therefore, provide an impressive array of potential information processing behaviors.

Acknowledgements. The authors would like to thank Xin Wang for providing reprints. This work was partially supported by Grant No. IBN-9634424 from the National Science Foundation.

References

Abarbanel HDI, Huerta R, Rabinovitch MI, Rulkov NF, Rowat PF, Selverston AI (1996) Synchronized action of synaptically coupled chaotic model neurons. Neural Comp 8:1567–1602

Abeles M (1991) Corticonics: neural circuits of the cerebral cortex. Cambridge University Press, New York

Adachi M, Aihara K (1997) Associative dynamics in a chaotic neural network. Neural Netw 10:83–98

Aihara K, Takabe T, Toyoda M (1990) Chaotic neural networks. Phys Lett A 144:333–340

Baird B (1986) Nonlinear dynamics of pattern formation and pattern recognition in the rabbit olfactory bulb. Physica D 22:150–175

Brown R, Rulkov NF, Tufillaro NB (1994) Synchronization of chaotic systems: the effect of additive noise and drift in the dynamics of the driving. Phys Rev E 50:4488–4508

Buzsàki G, Eidelberg E (1982) Direct afferent excitation and long-term potentiation of hippocampal interneurons. J Neurophysiol 48:597–607

Buzsàki G, Leung LS, Vanderwolf CH (1983) Cellular bases of hippocampal EEG in the behaving rat. Brain Res Rev 6:139–171

Campbell S, Wang DL (1996) Synchronization and desynchronization in a network of locally couple Wilson-Cowan oscillators. IEEE Trans Neural Netw 7:541–554

Carroll TL, Pecora LM (1993) Cascading synchronized chaotic systems. Physica D 67:126–140

Cessac B, Doyon B, Quoy M, Samuelides M (1994) Mean-field equations, bifurcation map and route to chaos in discrete time neural networks. Physica D 74:24–44

Doyon B, Cessac B, Quoy M, Samuelides M (1993) Control of the transition to chaos in neural networks with random connectivity. Int J Bif Chaos 3:279–291

Doyon B, Cessac B, Quoy M, Samuelides M (1994) On bifurcations and chaos in random neural networks. Acta Biotheor 42:215–225

Eckhorn R, Bauer R, Jordan W, Brosch M, Munk M, Reitboeck RJ (1988) Coherent oscillations: a mechanism of feature linking in the visual cortex? Multiple electrode and correlation analysis in the cat. Biol Cybern 60:121–130

Eeckman FH, Freeman WJ (1986) The sigmoid nonlinearity in neural computation: an experimental approach. In: Denker JS (ed) Neural networks for computing. AIP, New York, pp 135–145

Engel AK, König P, Kreiter AK, Singer W (1991a) Synchronization of oscillatory neuronal responses between striate and extrastriate visual cortical areas of the cat. Proc Natl Acad Sci USA 88:6048–6052

Engel AK, König P, Kreiter AK, Singer W (1991b) Interhemispheric synchronization of oscillatory neuronal responses in cat visual cortex. Science 252:1177–1179

Freeman WJ (1979) Nonlinear dynamics of paleocortex manifested in the olfactory EEG. Biol Cybern 35:21–37

Fox SE, Ranck JB Jr (1981) Electrophysiological characteristics of hippocampal complex-spike cells and theta cells. Exp Brain Res 41:399–410

Fox SE, Wolfson S, Ranck JB Jr (1986) Hippocampal theta rhythm and the firing of neurons in walking and urethane anesthetized rats. Exp Brain Res 62:495–508

Gray CM, König P, Engel AK, Singer W (1989) Oscillatory responses in cat visual cortex exhibit intercolumnar synchronization which reflects global stimulus properties. Nature 338:334–337

Grebogi C, Ott E, Yorke JA (1983) Crises, sudden changes in chaotic attractors, and transient chaos. Physica D 7:181–200

Hansel D, Sompolinsky H (1992) Synchronization and computation in a chaotic neural network. Phys Rev Lett 68:718–721

He R, Vaidya PG (1992) Analysis and synthesis of synchronous periodic and chaotic systems. Phys Rev A 46:7387–7392

Hertz J, Krogh A, Palmer RG (1991) Introduction to the theory of neural computation. Addison-Wesley, Redwood City, Calif

Hodgkin AL, Huxley AF (1952) A quantitative description of membrane current and its application to conduction and excitation in the nerve. J Physiol (Lond) 117:500–544

Hopfield JJ (1982) Neural networks and physical systems with emergent collective computational abilities. Proc Natl Acad Sci USA 79:2554–2558

Ishii S, Fukumizu K, Watanabe S (1996) A network of chaotic elements for information processing. Neural Networks 9:25–40

Kaneko K (1989) Spatiotemporal chaos in one- and two-dimensional coupled map lattices. Physica D 37:60–82

Kaneko K (1990) Clustering coding switching hierarchical ordering and control in a network of chaotic elements. Physica D 41:137–172

Kohonen T (1984) Self-organization and associative memory. Springer, Berlin Heidelberg New York

König P, Schillen TB (1991) Stimulus-dependent assembly formation of oscillatory responses. I. Synchronization. Neural Comput 3:155–166

Levine DS (1991) Introduction to neural and cognitive modeling. Lawrence Erlbaum, Hillsdale, NJ

Levy WB (1996) The sequence predicting CA3 is a flexible associator that learns and uses contexts to solve hippocampal-like tasks. Hippocampus 6:579–590

Macrides F, Eichenbaum H, Forbes WB (1982) Temporal relationship between sniffing and limbic theta rhythm during odor discrimination reversal learning. J Neurosci 2:1705–1717

Malescio G (1996) Noise and synchronization in chaotic systems. Phys Rev E 53:6551–6554

Malsburg C von der, Schneider W (1986) A neural cocktail-party processor. Biol Cybern 54:29–40

Malsburg C von der, Buhmann J (1992) Sensory segmentation with coupled neural oscillators. Biol Cybern 67:233–246

Minai AA, Anand T (1998a) Chaos-induced synchronization in discrete-time oscillators driven by a random input. Phys Rev E 57:1559–1562

Minai AA, Anand T (1998b) Using noise to synchronize chaotic neural oscillators. Proc IJCNN 98:1466–1471

Minai AA, Levy WB (1993) The dynamics of sparse random networks. Biol Cybern 70:177–187

Minai AA, Levy WB (1994) Setting the activity level in sparse random networks. Neural Comput 6:85–99

Minai AA, Pandian TD (1998) Communicating with noise: how chaos and noise combine to generate secure encryption keys. Chaos (in press)

Morgül Ö, Feki M (1997) Synchronization of chaotic systems by using occasional coupling. Phys Rev E 55:5004–5010

Murray JD (1989) Mathematical biology. Springer, Berlin Heidelberg New York

Pecora LM, Carroll TL (1990) Synchronization in chaotic systems. Phys Rev Lett 64:821–824

Pecora LM, Carroll TL (1991) Driving systems with chaotic signals. Phys Rev A 44:2374–2383

Peitgen H-O, Jürgens H, Saupe D (1992) Chaos and fractals: new frontiers of science. Springer, New York Berlin Heidelberg

Rall W (1955) Experimental monosynaptic input output relations in the mammalian spinal cord. J Cell Comp Physiol 46:413–437

Schillen TB, König P (1991) Stimulus-dependent assembly formation of oscillatory responses. II. Desynchronization Neural Comput 3:167–178

Skarda CA, Freeman WJ (1987) How brains make chaos in order to make sense of the world. Behav Brain Sci 10:161–195

Wang DL, Terman D (1995) Locally excitatory globally inhibitory oscillator networks. IEEE Trans Neural Networks 6:283–286

Wang X (1991) Period-doublings to chaos in a simple neural network: an analytic proof. Complex Syst 5:425–441

Wang X (1992) Discrete-time neural networks as dynamical systems. PhD Dissertation, University of Southern California

Wang X, Blum EK (1992) Discrete-time versus continuous-time models of neural networks. J Comput Syst Sci 45:1–19

Wilson HR, Cowan JD (1972) Excitatory and inhibitory interactions in localized populations. Biophys J 12:1–24

Wu X, Baxter RA, Levy WB (1996) Context codes and the effect of noisy learning on a simplified hippocampal CA3 model. Biol Cybern 74:159–165

Yao Y, Freeman WJ (1990) Model of biological pattern recognition with spatially chaotic dynamics. Neural Netw 3:153–170